EVS26
Los Angeles, California, May 6-9, 2012

Electrochemical-Calorimetric Studies on the Thermal Characteristics of $LiFePO_4$/graphite Cell

Jeff Q. Xu
Southwest Research Institute, San Antonio, TX 78228-0510, jeff.xu@swri.org

Abstract

The heat generation for lithium ion cell containing $LiFePO_4$ as cathode and graphite as anode at different charge/discharge rates is compared. The experimental measurement was made using an isothermal calorimeter consisting of a copper chamber maintained at 25 ^{0}C and cell temperature was held constantly at 40 ^{0}C in the middle of chamber. The heat generation was calculated from the subtraction of cell heat power with baseline power at 40 ^{0}C during cell rest period. Endothermic heating at the beginning of charge was apparent at different charging rates, and exothermic heating began quickly at less than 10% state of charge (SOC). The exothermic heating trend was continuing until the 100% SOC, but the heating profile was interesting at each SOC. During discharge, the rate of heat generation increased with increase in the discharge rates. The maximum heat generated at C/5 and C/2 discharging rates were ~0.54 W and ~0.17 W, respectively. The thermoneutral potentials were also calculated following thermodynamic equations, and the results showed variability for different charge and discharge rates. Commercially available 26650 format cylindrical cell was used for this research.

Keywords: $LiFePO_4$, heat generation, calorimeter, intercalation

1 Introduction

The lithium ion (Li-ion) battery is an emerging technology and has recently become a viable solution as an energy storage system for hybrid electric vehicle (HEV), plug-in hybrid electric vehicle (PHEV), and pure electric vehicle (EV). Presently Li-ion batteries are widely used in consumer electronics such as cell phones, laptop computers, and other small handheld devices. Further improvements for Li-ion battery technology are required to successfully implement Li-ion technology in electric vehicles. Common cathode materials include $LiCoO_2$, $LiNiO_2$, $LiMn_2O_4$, $LiFePO_4$, and $Li(Ni_{1/3}Co_{1/3}Mn_{1/3})O_2$. The anode of Li-ion batteries commonly uses carbonaceous materials, but more recently silicon and $Li_4Ti_5O_{12}$ have also been investigated [1]. Olivine-type $LiFePO_4$ is regarded as one of the most promising alternative cathode materials for Li-ion batteries because of its advantages of higher theoretic capacity (170 mAh/g), lower cost, higher safety, and environmental friendliness [2, 3]. Cathode and anode materials are coated and calenered on the metal foils during cell fabrication stage to form porous electrode. The porous electrodes consist of active cathode or anode material particles, binders, and other additives. The porous configuration of electrodes provides a high surface area for reactions and reduces the distance between reactants and the surface where reactions occur. Many novel materials for cathode, anode, electrolyte, and separator have been synthesized and evaluated to improve cell performance, life, safety, and cost.

Although Li-ion batteries have many attractive features, their possible application is still limited by safety concerns. Uncontrolled heat generation in the cell takes place under conditions such as high charge/discharge rates, operating at high environment temperatures, internal short circuit causing hot spots, and component failure. Under these conditions, thermally induced exothermic chemical reactions between the cell components

may be accelerated. Buildup of temperature gradients and solvent decomposition of electrolyte materials can lead to thermal runaway subsequently, with venting of gas, burning, and battery rupture. To overcome these safety problems, battery developers work to optimize cell designs and prescribe safe ranges of cell operating parameters. To optimize the cell design, sophisticated mathematical models have been developed based on specific assumptions about heat generation and thermal properties of various Li-ion batteries. However, the experimental heat generation rate data available in the public domain is very limited to $LiFePO_4$ cathode based cell chemistry. In this work, we report detailed experimental thermo-electrochemical data for a commercially available cylindrical LFP26650 Li-ion cell (3.0 Ah nominal capacity).

2 Experimental

2.1 Cell Selection

The cell selected for this study was commercially available LFP26650 cylindrical cell that uses $LiFePO_4$ as cathode and graphite as anode. The nominal capacity and voltage are 3.0 Ah and 3.2 V. The suggested discharge operation temperature range is between -25 ^{0}C and +55 ^{0}C.

2.2 Calorimeter

The tests were carried out on a PHI-TEC BTC battery tester calorimeter from HEL Group comprising voltage, current and temperature measurements, and a computer interface. This is a trolley mounted adiabatic calorimeter, which can be used for screening batteries and other larger samples and simulating the way in which exothermic self-heating and battery decomposition may occur. The sample sits at the heart of the calorimeter which is surrounded by metal guard heaters. The BTC guard heaters can track temperatures in excess of 10 ^{0}C min^{-1} and can reach temperatures of up to ~400 ^{0}C. In this research, Li-ion cell was maintained constantly at 40 ^{0}C and three guard heaters were maintained at either 25 ^{0}C or 30 ^{0}C. Battery charge/discharge steps were done separately by a Bitrode battery cycler. Table 1 summarizes the temperature setup for the calorimeter at two different charge/discharge rates. Fig. 1 shows the experimental setup.

Table 1: Key Parameters of Experimental Setup

	C/5 Charge/ Discharge Rate	C/2 Charge/ Discharge Rate
Cell Temperature (^{0}C)	40	40
Guard Heater Temperature Set (^{0}C)	30	25
Current (A)	0.6	1.5

Figure 1: Calorimeter and Cell Arrangement for Testing the Li-ion Cell on the PHI-TEC BTC

2.3 Experimental Process

The Li-ion cell was both charged and discharged at C/5 and C/2 rates. The charge process was under the following step: (1) the cell was charged at a constant current of either C/5 or C/2 rate to 3.7 V; (2) the cell voltage was held constant at 3.7 V until the current dropped to 0.09 A. The cell was discharged according to the following step: (1) the cell was rested for 2 hours at 40 ^{0}C before discharge; (2) the cell was discharged at either C/5 or C/2 rate down to 2.5 V.

3 Results and Discussion

3.1 Charging and Discharging Characteristics of Li-Ion Battery

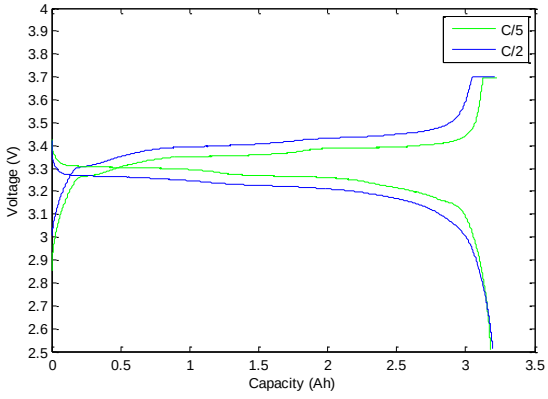

Figure 2: Capacity and Voltage

Fig. 2 compares the voltage curves of tested Li-ion cell at C/5 and C/2 for charging and discharging. As one of important steps in thermal analysis, the capacity and voltage behavior of the cell must be determined. Charging was done galvanostatically until the cell voltage reached 3.7 V, then the constant voltage (3.7 V) was held to allow the current dropped to a pre-set value as described above. Discharging was done galvanostatically only. Fig. 2 shows the charging and discharging voltage profiles for the C/5 and C/2 rates at 40 ^{0}C inside the calorimeter. Table 2 summarizes the capacity of cell charged by constant current (CC) and by constant current (CC) plus constant voltage (CV). Total charging capacity for two rates is very close and the difference is 0.0125 Ah which is less than 0.4% from the average. One of interesting data is the percentage of CC charging versus total capacity combined CC and CV charging. CC charging for C/5 rate is almost 97% of total charging capacity and is nearly 2% higher than CC charging at C/2 rate. This phenomenon can be attributed to over-potential polarization at relatively high charging rate. The discharging capacity for two rates is also very close and the difference is 0.0157 Ah which is less than 0.5% from the average.

Table 3 summarizes the open circuit voltages (OCV) before charging and discharging for the C/5 and C/2. The table also lists the discharge voltages when the cell was discharged at 50% depth of discharge (DOD). This can be considered to be a mid–discharge voltage indication, and the voltage at C/5 discharging rate is 43 mV higher than at C/2 rate. This can also be attributed to the polarization.

Table 2: Cell Capacity of Charging and Discharging

	CC Charging (Ah)	CC+CV Charging (Ah)	CC/ (CC+CV) Charging	CC Discharging (Ah)
C/5	3.1262	3.2259	96.91%	3.1799
C/2	3.0515	3.2134	94.96%	3.1956

Table 3: Cell Voltage of Charging and Discharging

	OCV before Charging (V)	OCV before Discharging (V)	Discharge Voltage @ 50% DOD (V)
C/5	2.854	3.429	3.267
C/2	2.920	3.425	3.224

3.2 Heat Generation

Heat generation during cell discharge and charge is of concern not only for the safety reason, but also for extending the cell cycle and calendar life. In addition, it is important to know whether the battery cell is susceptible to thermal runaway when the rate of heat generated exceeds the rate of heat dissipated, especially when the cells are connected in series and parallel as a module or pack for HEV/PHEV/EV applications. Another thermal effect that affects cell operation is the result of thermal gradients and hot spots inside the cell when the cell is under charging or discharging, which greatly accelerates degradation of the electrolyte, electrode materials for anode and cathode, separator, current collector, and packaging materials. The thermal characterization of Li-ion cells is complex and difficult due to uncertainty regarding cathode and anode reaction mechanisms, side reactions, and cell design.

Viswanathan et al. have analyzed the reversible and irreversible heat of Li-ion batteries during charge and discharge process [4]. A battery cell releases and absorbs heat during charge and discharge reactions. If the cell electrode reaction progresses in reverse, then the discharge and charge reactions are the reverse of one another, and so the intake and release of heat is reversed as well. This can be considered as a reversible reaction, which is dependent on cell chemistry exclusively. In this typical experimental cell chemistry, the overall electrochemical reaction for charging and discharging can be described as:

$LiFePO_4 + 6C = FePO_4 + LiC_6$ (fully charged)
$LiC_6 + FePO_4 = LiFePO_4 + 6C$ (fully discharged)
$Li_xFePO_4 + 6C = Li_{1-x}FePO_4 + LixC_6$
(charging and discharging in process)

The reversible reaction heat value Qr can be expressed with Equation 1.

$$Qr = T\Delta S(I/nF) \quad (1)$$

where I is the current (A), T is temperature (K), ΔS is entropy change (J mol^{-1} K^{-1}), n equals the number of electrons per reaction, and F is the Faraday constant. Based on one Li exchange during charge or discharge, the entropy change is given by

$$\Delta S = nF(\partial E/\partial T) \quad (2)$$

where E is the open circuit voltage (OCV). The battery reaction also results in side reactions and self-discharges due to electrolyte decomposition, which is manifested as thermal factor Qs. When battery cell is under load, its internal resistance

caused by Ohmic polarization, mass transfer polarization, and diffusion polarization will be contributed to Joule heat Qp, which is an irreversible heat loss. Total heat generation in the battery cell charging and discharging, Qt, is therefore expressed with Eq. 3:

$$Qt = Qr + Qs + Qp \qquad (3)$$

During charging, the reaction heat Qr in a Li-ion battery corresponds to the heat absorbed or released when lithium ions are de-intercalated at the positive electrode (cathode) and intercalated at the negative electrode (anode). In addition, a quantity of heat equivalent to this process is generated or absorbed during discharging process. Through previous research [4, 5, 6], this process is cell chemistry depended.

In addition, Qs produced by battery cell side reactions and self-discharge is relatively small during a single time charging or discharging process compared with Qr and Qp. Therefore, the total heat generated, Qt, can be expressed as:

$$Qt = Qr + Qp \qquad (4)$$

3.3 Heat Generation Profile

Fig. 3 (a) and (b) are heat profiles of experimental cell charging and discharging under C/5 and C/2 rates, respectively. From both graphs, one can see there is a distinct heat profile at different charging and discharging timeframe. At C/5 and C/2 rates, the baselines of cell heater power were ~0.7 W and ~1.0 W, respectively. The power data in the Fig. 3 (a) and (b) are five times of raw data to offer the same scale as voltage data. Both endothermic and exothermic phenomena can be seen clearly from the graphs, although the heat profile at C/5 rate has a lot of noise oscillation due to the instrumentation setup.

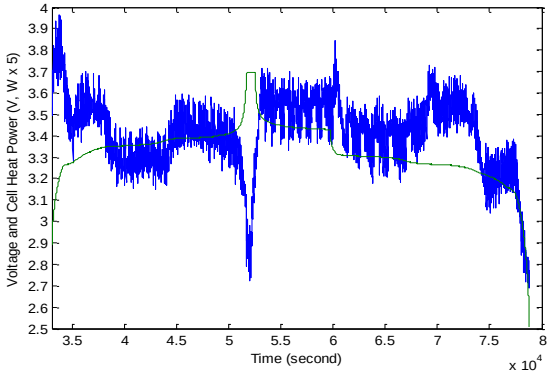

(a)

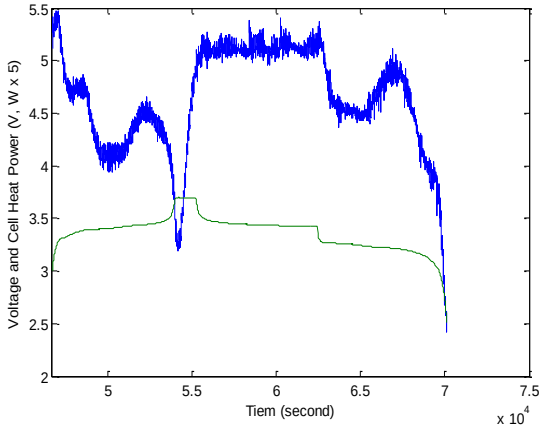

(b)

Figure 3: Heat Generation and Voltage Profile. (a) C/5 (power x5); (b) C/2 (power x 5)

Fig. 4 (a) is the cell heat generation versus the state of charge (SOC) at charging and discharging under C/5 rate cycling. Fig. 4 (b) is the cell heat generation versus the state of charge (SOC) at charging and discharging under C/2 rate cycling. From the graphs, five distinct heat regions can be seen that demonstrate five different lithium ion de-intercalation and intercalation mechanisms. The five regions can be categorized as:

Region 1: <10% SOC
Region 2: ~10% - 30% SOC
Region 3: ~30% - 60% SOC
Region 4: ~60% - 90% SOC
Region 5: >90% SOC

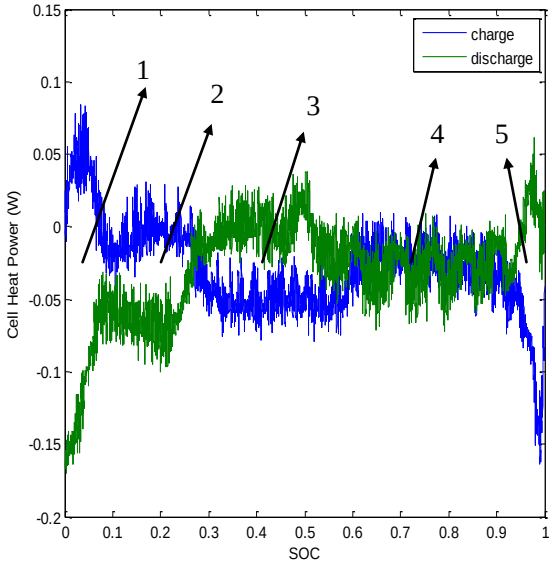

(a)

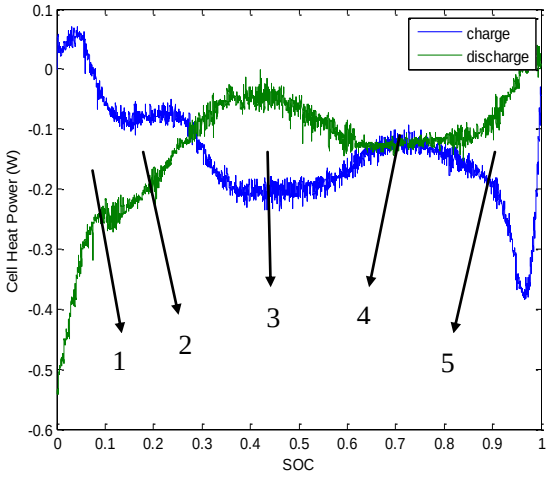

(b)

Figure 4: Cell Heat Power versus the State of Charge (SOC).
(a) C/5 charging and discharging rate;
(b) C/2 charging and discharging rate

To our knowledge, there are no literatures reported for $LiFePO_4$ cell chemistry to address the intercalation and de-intercalation mechanisms in above-proposed five regions. At the beginning of charge, there is an endothermic peak. One can attribute this endothermic peak to the $LiFePO_4$ de-intercalation. Literature [4] has reported that lithium ion intercalation into graphite is an exothermically dominated process. Since the heat profile was acquired from a full cell battery, it is difficult to differentiate whether the heat is generated from either lithium ion de-intercalation/intercalation from $LiFePO_4$ or lithium ion intercalation/de-intercalation from graphite during charging/discharging process. In general, heat profile at charging and discharging process is very much reversible except the Region 1 and Region 5.

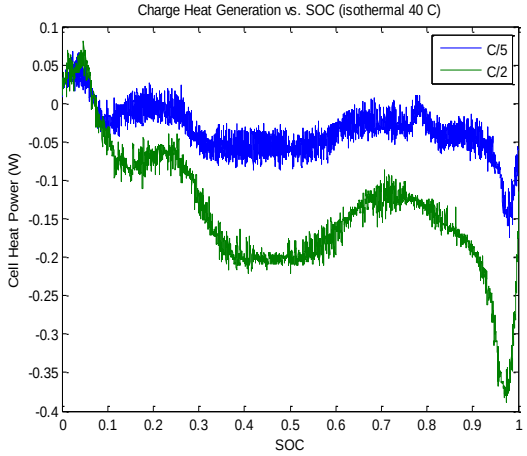

(a)

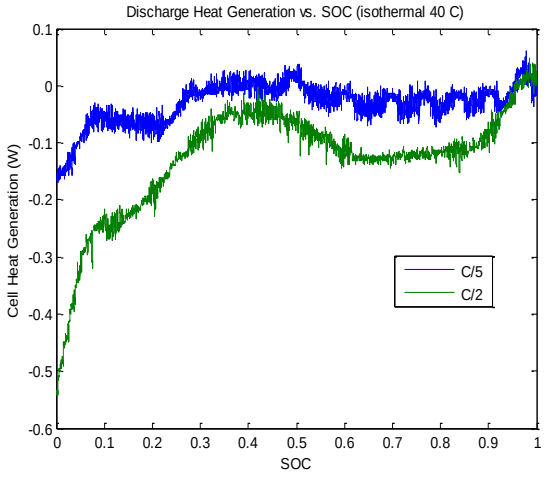

(b)

Figure 5: Cell Heat Power Trend versus the State of Charge (SOC) at Charge/Discharge.
(a) Charge at C/5 and C/2 Rates
(b) Discharge at C/5 and C/2 Rates

Fig. 5 (a) and (b) show the heat generation profiles of charge and discharge at C/5 and C/2 rates. Both graphs offer the same heat generation trend for two different rates. The maximum heat generated at C/5 and C/2 discharging rates were ~0.51 W and ~0.17 W, respectively.

3.4 Thermoneutral Potential

Generally, thermoneutral potential can be used to calculate heat generation under various operating conditions, based on known voltage profiles during charge and discharge. As we know, Qp can be expressed as:

$$Qp = -nF(E - E_{load}) \qquad (5)$$

E is the open circuit voltage, and E_{load} is the voltage under load. So, Equation (4) can be expressed through combining Equation (1) and (2):

$$Qt = -nF\,[E - E_{load} - T(\partial E/\partial T)] \qquad (6)$$

From thermodynamics, we know that thermoneutral potential (E_H) of electrochemical reaction is:

$$E_H = -(\Delta Hr/nF) = E - T(\partial E/\partial T)] \qquad (7)$$

ΔHr is the enthalpy change of electrochemical reaction, therefore,

$$Qt = -nF\,(E_H - E_{load}) \qquad (8)$$

$$E_H = (-Qt/nF) + E_{load} \qquad (9)$$

$$E_H = (-Qt/I) + E_{load} \quad (10)$$

Qt is in Watt at Equation (10)

Table 4 summarizes all different trial calculations to obtain a more representative voltage for this specific cell chemistry.

Table 4: Calculated Values for E_H

Test Regime	Value to E_H (V)
C/5 charge rate 0-100% SOC range	3.427
C/5 charge rate 10-90% SOC range	3.423
C/5 discharge rate 0-100% SOC range	3.294
C/5 discharge rate 10-90% SOC range	3.306
C/2 charge rate 0-100% SOC range	3.686
C/2 charge rate 10-90% SOC range	3.649
C/2 discharge rate 0-100% SOC range	3.405
C/2 discharge rate 10-90% SOC range	3.406
Average	**3.450**

The calculations suggest an average value of 3.450 V for E_H was given in Table 4. Obviously, the value from C/5 rate seems smaller than the value from C/2 rate. The reason for the variability of resulted value is still unknown and needs to be investigated further.

4 Conclusion

The heat generation for Li-ion cell containing $LiFePO_4$ as cathode and graphite as anode at different charge/discharge rates is compared. The experimental measurement was made using an isothermal calorimeter consisting of a copper chamber maintained at 25 ^{0}C and cell temperature was held constantly at 40 ^{0}C in the middle of chamber. The heat generation was calculated from the subtraction of cell heat power with baseline power at 40 ^{0}C during cell rest period. Endothermic heating at the beginning of charge was apparent at different charging rates, and exothermic heating began quickly at less than 10% state of charge (SOC). The exothermic heating trend was continuing until the 100% SOC, but the heating profile was interesting at each SOC. During discharge, the rate of heat generation increased with increase in the discharge rates. The maximum heat generated at C/5 and C/2 discharging rates were ~0.51 W and ~0.17 W, respectively. The thermoneutral potentials were also calculated following thermodynamic equations, and the results showed variability for different charge and discharge rates. Commercially available 26650 format cylindrical cell was used for this research.

Acknowledgments

This study is supported by the internal research and development (IR&D) program of Southwest Research Institute (Project # 03-63799). The author is grateful to Karl Kreder for the experimental setup and data collection. The Author would like to acknowledge energy storage system evaluation and safety (EssEs) consortium for the experimental instrumentation. Also sincerely appreciate the helpful discussion and support from Dr. Jayant Sarlashkar and Cheuk Ng.

References

[1] J.B. Goodenough and Y. Kim, “Challenges for Rechargeable Li Batteries”, Chem. Mater., 2010, 22 (3), pp 587–603.

[2] A. Du Pasquier, A. Laforgue, P. Simon, G.G. Amatucci, and Jean-Francois Fauvarqueb, “Nonaqueous Asymmetric Hybrid Li4Ti5O12/Poly(fluorophenylthiophene) Energy Storage Device”, J of The Electrochemical Society, 149 (3), A302-A306 (2002).

[3] A.K. Padhi, K.S. Nanjundaswamy, J.B. Goodenough,"$LiFePO_4$: A Novel Cathode Material for Rechargeable Batteries", Electrochemical Society Meeting Abstracts, **96-1**, May, 1996, pp 73.

[4] V.V. Viswanathan, D. Choi, D. Wang, W. Xu, S. Towne, R.E. Williford, J. Zhang, J. Liu, and Z. Yang, “Effect of entropy change of lithium intercalation in cathodes and anodes on Li-ion battery thermal management”, J Power Sources. 2010; 195:3720–9.

[5] Y. Kobayashi, H. Miyashiro, K. Kumai, K. Takei, T. Iwahori, and I. Uchida,

"Precise Electrochemical Calorimetry of $LiCoO_2$/Graphite Lithium-ion Cell", J of The Electrochemical Society, 149 (8) A978-A982 (2002).

[6] Y. Kobayashi, N.Kihira, K. Takei, H. Miyashiro, K. Kumai, N. Terada, R. Ishikawa, "Electrochemical and Calorimetric Approach to Spinel Lithium Manganese Oxide", J Power Sources. 1999; 81-82:463–466.

Author

Mr. Jeff Xu received MS in chemistry and MBA in management of technology from Simon Fraser University, Canada in 1999 and 2001. He also received MS in analytical chemistry at Xiamen University in 1989. He joined Southwest Research Institute as a principal scientist to assist electric vehicle development program consisting of battery testing activities and internal research program. He is a member of Society of Automotive Engineering (SAE) and American Chemical Society (ACS).